Hindawi
Complexity
Volume 2024, Article ID 9846948, 1 page
https://doi.org/10.1155/2024/9846948

Retraction

Retracted: Explosion Resistance of Three-Dimensional Mesoscopic Model of Complex Closed-Cell Aluminum Foam Sandwich Structure Based on Random Generation Algorithm

Complexity

Received 23 January 2024; Accepted 23 January 2024; Published 24 January 2024

This article has been retracted by Hindawi following an investigation undertaken by the publisher [1]. This investigation has uncovered evidence of one or more of the following indicators of systematic manipulation of the publication process:

(1) Discrepancies in scope

(2) Discrepancies in the description of the research reported

(3) Discrepancies between the availability of data and the research described

(4) Inappropriate citations

(5) Incoherent, meaningless and/or irrelevant content included in the article

(6) Manipulated or compromised peer review

The presence of these indicators undermines our confidence in the integrity of the article's content and we cannot, therefore, vouch for its reliability. Please note that this notice is intended solely to alert readers that the content of this article is unreliable. We have not investigated whether authors were aware of or involved in the systematic manipulation of the publication process.

Wiley and Hindawi regrets that the usual quality checks did not identify these issues before publication and have since put additional measures in place to safeguard research integrity.

We wish to credit our own Research Integrity and Research Publishing teams and anonymous and named external researchers and research integrity experts for contributing to this investigation.

The corresponding author, as the representative of all authors, has been given the opportunity to register their agreement or disagreement to this retraction. We have kept a record of any response received.

References

[1] Z. Wang, W. B. Gu, X. B. Xie, Q. Yuan, Y. T. Chen, and T. Jiang, "Explosion Resistance of Three-Dimensional Mesoscopic Model of Complex Closed-Cell Aluminum Foam Sandwich Structure Based on Random Generation Algorithm," *Complexity*, vol. 2020, Article ID 8390798, 16 pages, 2020.

Hindawi
Complexity
Volume 2020, Article ID 8390798, 16 pages
https://doi.org/10.1155/2020/8390798

Research Article

Explosion Resistance of Three-Dimensional Mesoscopic Model of Complex Closed-Cell Aluminum Foam Sandwich Structure Based on Random Generation Algorithm

Zhen Wang, Wen Bin Gu, Xing Bo Xie, Qi Yuan, Yu Tian Chen, and Tao Jiang

Army Engineering University of PLA, Nanjing 210007, China

Correspondence should be addressed to Wen Bin Gu; 1120122090@bit.edu.cn

Received 1 June 2020; Accepted 11 July 2020; Published 29 July 2020

Guest Editor: Zhihan Lv

According to the randomness of the spatial distribution and shape of the internal cells of closed-cell foam aluminum and based on the Voronoi algorithm, we use ABAQUS to model the random polyhedrons of pore cells firstly. Then, the algorithm of generating aluminum foam with random pore size and random wall thickness is written by Python and Fortran, and the mesh model of random polyhedral particles and random wall thickness was established by the algorithm read in by TrueGrid software. Finally, the mesh model is impo rted into the LS-DYNA software to remove the random polyhedron part of the pore cell. Compared with the results of scanning electron microscopy and antiknock test, the morphology and properties of the model are close to those of the real aluminum foam material, and the coincidence degree is more than 91.4%. By means of numerical simulation, the mechanism of the wall deformation, destruction of closed-cell aluminum foams, and the rapid attenuation of explosion stress wave after the interference of reflection and transmission of bubbles were studied and revealed. It is found that aluminum foam deformation can be divided into four areas: collapse area, fracture area, plastic deformation area, and elastic deformation region. Therefore, the explosion resistance is directly related to the cell wall thickness and bubble size, and there is an optimal porosity rule for aluminum foam antiknock performance.

1. Introduction

Closed-cell aluminum foams are a kind of porous metal material, which is composed of thousands of random 3D polyhedral pores embedded in continuous aluminum or aluminum alloy matrix. Compared with other composites, closed-cell aluminum foam has the characteristics of lightweight, high strength, and dual physical properties of function and structure. Because of its unique mesostructural characteristics, the material can have long and almost constant platform stress in compression, which is very beneficial for energy absorption [1, 2]. Therefore, aluminum foams are being increasingly used in energy-absorbing structures [3–11]. It has been widely used in the field of explosion and impact protection. Goel et al. [12] studied the effect of closed-cell aluminum foam on the shock wave passing through the impact tube, and it is found that the existence of aluminum foam interlayer has a great influence on the reflected wave. According to the research of Shen et al. [13], they carried out the explosion loading experiment on the aluminum foam sandwich plate which was bent outwards and found that compared with the plane aluminum foam sandwich plate, this structure changed the incident angle of detonation wave and the deformation mechanism of the panel. Its antiknock ability was better than the latter. Jing et al. [14–16] introduced experimental studies on antiknock performance of circular arc foam metal composite panels, and the deformation and failure characteristics of such composite plates subjected to blast loading are analyzed.

As we all know, the local failure and deformation of aluminum foam are very serious under the condition of a strong dynamic load. It is difficult to obtain the local mesofailure mode and the failure process (mode) of deformation, collapse, and fracture in the experimental study. Some studies have shown that the mechanical properties of

aluminum foam materials show obvious multiscale characteristics [17]. At the mesolevel, the mechanical behaviors of the aluminum foam cell wall, such as plastic deformation, buckling, and fracture, have a great influence on the macromechanical properties. Therefore, scholars at home and abroad have established a large number of numerical models and carried out a variety of research methods [18–23].

At present, there are three main methods to study the mesoscopic model of porous metal materials. The first method adopts repeating unit cell (RUC). The macromechanical properties and deformation characteristics of aluminum foam structure are simulated by regularly repeating the predesigned representative unit. The choice of representative units is more diversified. Gibson and Ashby [24] proposed a cubic structure model for closed-cell foam materials. It assumes that the cell structure is a simple and repeated arrangement of cubes, the edge length, edge wall, and wall thickness of each cube are the same, and the elastic modulus and yield strength expression of the foam material are given by this model. In order to more realistically simulate the cell structure of actual aluminum foam, the basic unit shape of this representative model has also been gradually improved. Representative models of closed-cell aluminum foam have successively developed such ideal models as the Kalman model (tetrahedral model) [20, 25, 26], octahedral model [27], more complex cube to pyramid model [28], cube to sphere model [28, 29], all of which use uniform pores, cell walls, and prisms. The main drawback of this method is that it cannot reflect the randomness of the microstructure of aluminum foam. The second type of method considers the randomness of the microstructure of aluminum foam on this basis and generates a cell structure to simulate the pore structure of aluminum foam by certain rules. Many scholars [19, 31, 32] proposed a three-dimensional Voronoi algorithm technology to establish foam three-dimensional mesoscopic model of aluminum. This model can reflect the mesomechanical properties of aluminum foam more realistically, and it has great significance for the study of its energy dissipation mechanism and deformation mode. However, most of the hole walls use shell elements, and their thickness is the same at any position, which is obviously not consistent with the experimental observation results. The third type of method is to perform three-dimensional reconstruction based on the CT scan image of the material to obtain the mesofinite element model [3], which can truly restore the mesoscopic structural characteristics of aluminum foam. However, the number of finite element model elements obtained by this method is huge, and the calculation cost is far more than the previous two methods. In order to more realistically simulate the deformation and failure process of aluminum foam under external load, it is necessary to establish a cell wall model of aluminum foam in line with the actual situation to study the mechanical properties of aluminum foam. Fang et al. [33, 34] used a three-dimensional random polyhedron model algorithm to simulate foam metal materials. The pores were simulated using three-dimensional random convex polyhedrons. At the same time, a random control algorithm for wall thickness was proposed to achieve random distribution of pores and wall thickness but also increased the calculation of the amount. It is difficult to increase the porosity by a large margin, and there is no real explosive simulation.

In this paper, on the basis of the Voronoi algorithm, the process of random pore size and cell wall thickness is realized by self-programming. A closed-cell aluminum foams modeling method based on a three-dimensional mesomodel is proposed. This method greatly improves the calculation efficiency and shortens the calculation time. At the same time, the sandwich structure of the aluminum foam is designed, and the correctness of the three-dimensional micromodel of aluminum foam is verified by experiments. On the basis of the established finite element model of real structure, the deformation mode, energy absorption effect, and attenuation mechanism of explosion shock wave of aluminum foam sandwich structure were studied, and the wave attenuation law of aluminum foam to explosion loads with different porosities was obtained. These experimental results can provide a theoretical basis for the design of the weight reduction device.

2. Mesoscopic Model Setup

The microstructure of closed-cell foam aluminum has a large number of randomly distributed closed cells. In this chapter, we consider the cells in the foam, give the generation algorithm of the closed-cell foam aluminum three-dimensional model, and establish the three-dimensional mesoscopic model of the aluminum foam. The algorithm consists of three steps. The first is the generation of random polyhedron particles. The pores of aluminum foam are regarded as random polyhedral particles. Based on the Voronoi algorithm, ABAQUS is used to model the random polyhedrons and extract their geometric features. The second is to comprehensively use the Python language and Fortran language to write a three-dimensional random aluminum pore size and random wall thickness foam aluminum generation algorithm, so that the aluminum foam cell wall thickness is random, through the TrueGrid software reading algorithm, the establishment of random polyhedron particles, and random wall thickness grid model. The third is to import the mesh model into the LS-DYNA software, random polyhedron particle part of pore cell is removed, generate a foam aluminum model, and then build an explosion model of the foam aluminum sandwich panel.

2.1. Describe the Randomness of Pore Size and Cell Wall Thickness. The closed-cell foam metal is composed of a large number of randomly distributed closed cells and cell walls. The pore size is generally 0.5–4 mm, and the cell wall thickness is about 0.05–2 mm. The cell pore size and cell wall thickness are randomly distributed. Metal foams exhibit typical heterogeneity derived from the microstructure of the cell wall.

In this paper, the foam aluminum model algorithm is based on the Voronoi algorithm, using the Python language and Fortran language comprehensively. According to the

mesostructure characteristics of aluminum foam, the modeling method of complex polyhedron is partially improved to Voronoi algorithm. Consider randomness. It not only realizes the randomness of the pore size of the aluminum foam but also realizes the randomness of the wall thickness, so it is a more realistic mesoscopic model of the aluminum foam. The generation of cell walls and particles is shown in Figure 1:

According to the Voronoi algorithm, the discrete data points are reasonably connected to construct a Delaunay triangle network, and then the vertical bisectors of the line segments of two adjacent points are connected to form a Tyson polygon [34], as shown in the figure. Each vertex of the Tyson polygon is the circumscribed circle center of the adjacent triangle. The Tyson polygon is regarded as the pores of two-dimensional aluminum foam. By adjusting the number of polygons, the polygonal pore diameter is controlled within 1–3 mm, and the average pore diameter is 2 mm. Using the Python language and Fortran language comprehensively, a random algorithm of random cell wall thickness is written to obtain the cell wall as shown in Figure 1(b), and the size of the pore size is finely adjusted by the cell wall thickness. At this point, the geometric model of the two-dimensional aluminum foam and the cell wall is generated. After the algorithm is improved, it can be programmed with shorter sentences, which is highly executable, shortens the modeling running time, and generates models quickly.

Then, the two-dimensional model is extended to the three-dimensional cube domain, random polyhedrons are generated in the cubes of arbitrary shape and structure as shown in Figure 2, random thickness is given to any geometric surface by random algorithm, then the random thickness of the cell wall the value range is 0.03~0.4 mm, and the random function of the cell wall is as follows:

$$T_d = T_{\max} - \left(T_{\max} - T_{\min}\right) \times \zeta_{\text{random}}, \tag{1}$$

where T_{d} is the cell wall thickness, $T_{\min}$ and $T_{\max}$ are the minimum and maximum cell wall thickness, ζ_{random} is the random distribution function of the cell wall thickness, and the value range is 0~1. A suitable foam cell mesoscopic model should take into account the randomness of nonuniformity, pore size, and cell wall thickness. $T_{\min}$ and $T_{\max}$ were taken as 0.03 and 0.4 mm, respectively, until the cell wall thickness satisfies 0.03~0.4 mm to stop the regeneration of random polyhedron and finally get the three-dimensional polyhedron geometric model of Figure 2(b). Compared with other algorithms, this algorithm can effectively shorten the modeling time and improve the calculation efficiency and ensure the randomness of the cell wall and pore size.

2.2. Generation of Grid. Use TrueGrid software to read in the random pores and random cell wall foam aluminum algorithm, extract geometric features, and use the mapping grid method to build a grid model of random polyhedral particles and random wall thickness. Aiming at the characteristics of the pore delivery area of the closed-cell foam aluminum mesomodel, a structured grid is divided, and the characteristic size of the unit is determined according to the pore diameter and wall thickness. In order to take into account both the computational efficiency and the accuracy of the simulation, this paper takes the feature size of the cell as the grid size is set to 0.2 mm. The regular cell distribution characteristics ensure the calculation efficiency of the subsequent material judgment and are conducive to programming. A spatial eight-node hexahedral unit is used to divide the overall delivery area into a uniform grid to obtain a regular initial grid structure. A fine and uniform grid improves computational efficiency while ensuring accuracy. First build a cube model that surrounds the cylinder, as shown in Figure 3(a); then fill the extracted geometric features in Figure 3(a) to get Figure 3(b); according to the position of the grid in the sample, determine the material properties of the grid; when all nodes of the element are located in a random polyhedron, the material property is set to pore; otherwise, it is defined as aluminum material. Then perform cylindrical cutting to delete the aluminum foam model outside the cylinder, and the remaining part is shown in Figure 3(c); and then propose removing the particle model part and obtaining the mesh model of the foam aluminum as shown in Figure 3(d), the output grid file, the three-dimensional view of aluminum foam is shown in Figure 3(e). To facilitate the observation of the internal structure of aluminum foam, a quarter model is intercepted, as shown in Figure 3(f).

2.3. Modeling of Aluminum Foam Sandwich Structure. Use TrueGrid software to establish the air grid model and fill the air grid with explosives and the explosive and the air grid share nodes; use SCDM software to establish the geometric model of the sleeve, cover plate, and bottom plate; divide and export the *K* files of all fluid and solid grids; assemble the grids in the LS-PrePost software together with the *K* files of the aluminum foam; and finally obtain the model and *K* file of the aluminum foam sandwich structure. The quarter model and dimensions are shown in Figure 4. The size of the air domain is 0.82 m × 0.42 m × 0.4 mm, the radius of the explosive is 0.043 m, the thickness of the cover plate is 0.01 m, and the thickness of the bottom plate is 0.02 m.

Add a nonreflective boundary condition on the outer surface of the air layer, the bottom of the bottom plate is set as a fixed boundary, the cover plate and the bottom plate are bound and connected, *CONTACT_TIED_SURFACE_TO_SURFACE, the cover plate and the aluminum foam, and the aluminum foam and the bottom plate take automatic surface-to-surface contact *CONTACT_AUTOMATIC_SURFACE_TO_SURFACE.

In order to accurately analyze the nonlinear behavior of the foam aluminum sandwich panel under strong dynamic load, the system bottom plate, sleeve, bracket, and end cover are Q235 steel. The above materials and foam aluminum are all used in the PLASTIC KINEMATIC material model of LS-DYNA. The metal materials were numerically simulated. The calculation parameters of metal materials are shown in Table 1.

The air uses the *MAT_NULL material model, and the equation of state is described using *EOS_LINEAR_

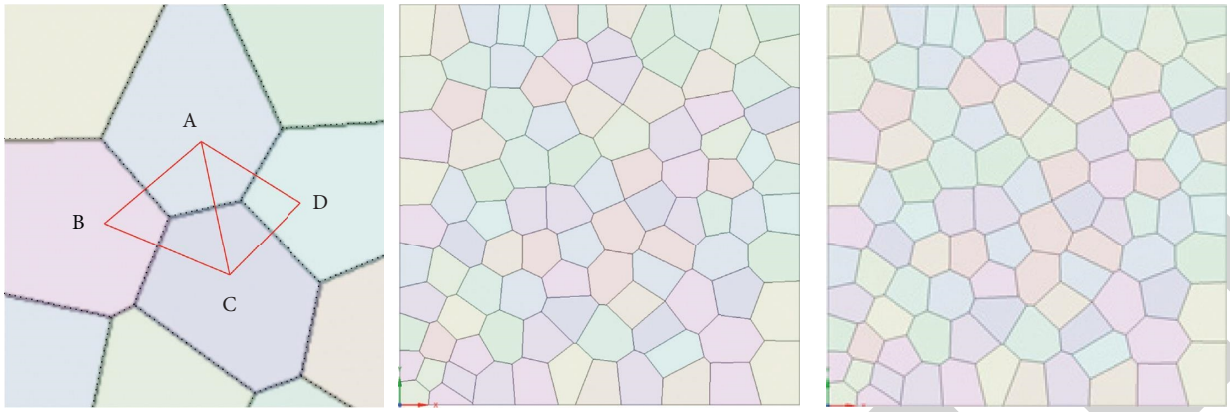

(a) (b)

Figure 1: Two-dimensional particle and cell wall generation process.

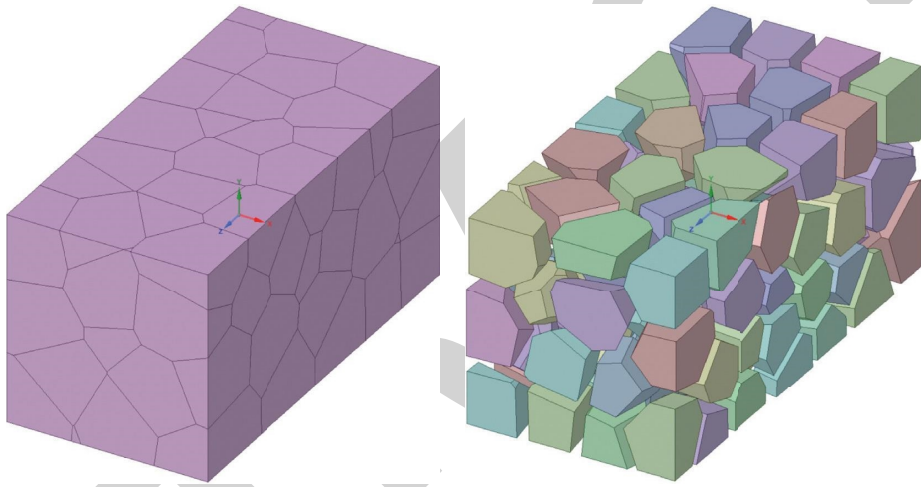

(a) (b)

Figure 2: Random polyhedron and cell wall generation process. (a) Random polyhedron generation. (b) Generation of three-dimensional cell wall model.

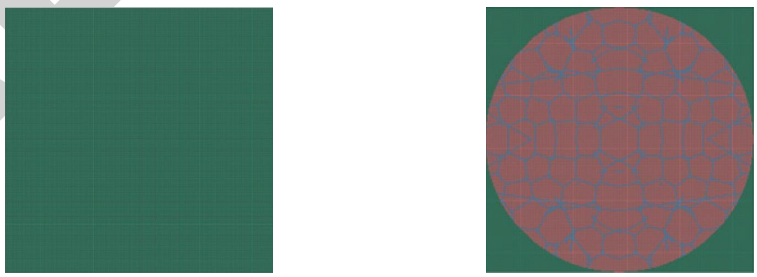

(a) (b)

Figure 3: Continued.

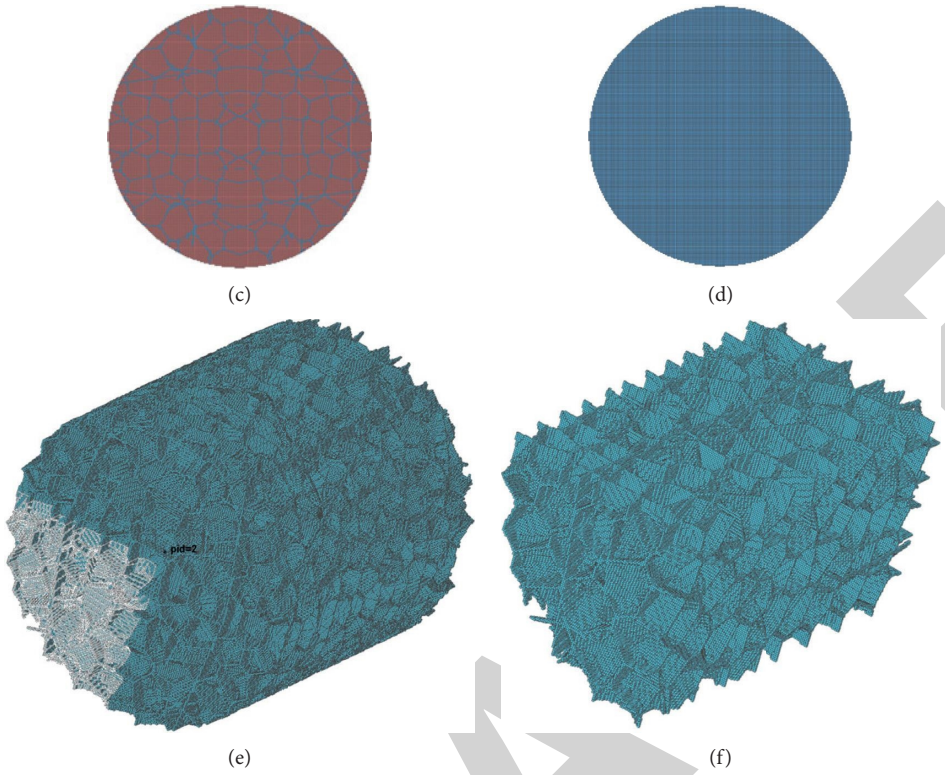

Figure 3: Finite element model generation of aluminum foam.

Table 1: Metal material parameters.

Metallic material	Q (kg/m^3)	E (GPa)	I	SIGY (MPa)	ETAN (GPa)
Q235 steel [35]	7830	210	0.274	235	6.1
Aluminum foam [33]	2730	70	0.34	185	4.62

POLYNOMIAL. The expression of the equation of state is as follows:

$$p = C_0 + C_1\mu + C_2\mu^2 + C_3\mu^3 + \left(C_4 + C_5\mu + C_6\mu^2\right)E,$$
$$\mu = \frac{1}{V} - 1 = \frac{\rho}{\rho_0} - 1, \quad (2)$$
$$C_4 = C_5 = \gamma - 1.$$

Considering air as a gas in an ideal state, the coefficients of the polynomial equation $C_0 = C_1 = C_2 = C_3 = C_6 = 0$. The variable coefficient γ is often set to 1.4, so $C_4 = C_5 = 0.4$. E_0, ρ_0, and V_0 which are the initial energy density, initial density, and initial relative volume parameter values are 1.29 g·cm^{-3}, 0.25 MPa, and 1.0. The parameters are shown in Table 2.

The high-energy combustion explosives use *MAT_HIGH_EXPLOSIVE_BURN material model, and the equation of state uses *EOS_JWL to represent the pressure of the explosive product. The expression of the equation of state is as follows:

$$p = A\left(1 - \frac{\omega}{R_1V}\right)e^{-R_1V} + B\left(1 - \frac{\omega}{R_2V}\right)e^{-R_2V} + \frac{\omega E}{V}, \quad (3)$$

Table 2: Air material parameters [22].

C_0 (MPa)	C_1	C_2	C_3	C_4	C_5	C_6	ρ (kg/m^3)
−0.1	0	0	0	0.4	0.4	0	1.225

where E and V are energy density and relative volume, respectively, and the initial values should be assigned to E_0; V_0, A, B, and E_0 are pressure units; and R_1, R_2, OMEG, and V_0 are dimensionless. The specific material parameters are shown in Table 3.

And use the ALE algorithm to solve *CONTROL_ALE, the explosive and air form an Euler multimatter group (*ALE_MULTI-MATERIAL_GROUP), and the fluid domain and solid domain are set by fluid-solid coupling (*CONSTRAINED_LAGRANGE_IN_SOLID). Finally submit ANSYS/LS-DYNA for solution.

In the geometric nonlinear analysis of explosion impact, the material often deforms greatly. In order to better fit the changing shape of the aluminum foam cell wall under real conditions, the material erosion method is often used to deal with the distorted unit. When the stress or strain reaches the erosion failure condition, we consider this element to fail and remove it from the model. The failure criterion of

Table 3: Explosive material parameters [36].

ρ (kg/m^3)	A (GPa)	B (GPa)	R_1	R_2	PCJ (GPa)	E (J/m^3)	D (m/s)	υ	ω
1500	347.6	3.39	4.15	0.95	17.92	6.34e9	6957.2	1.0	0.28

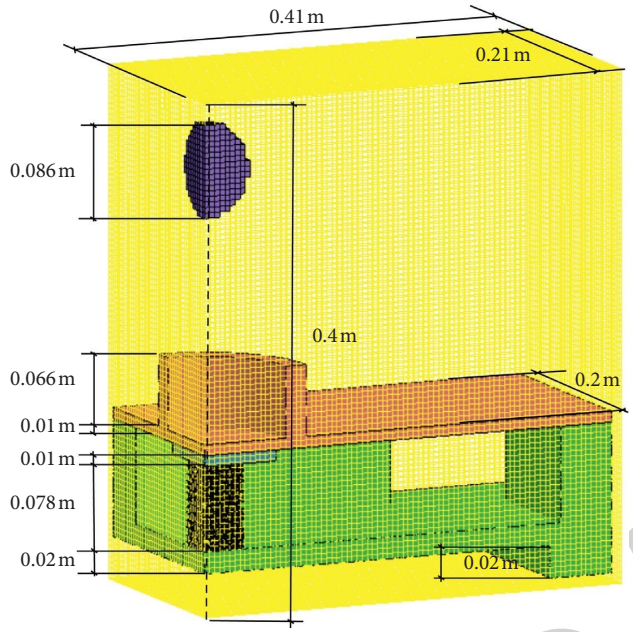

Figure 4: Sandwich plate model.

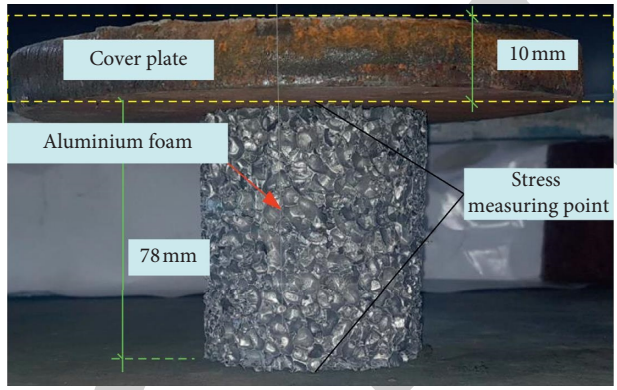

Figure 5: Sandwich plate antiexplosion test device.

aluminum foam adopts the maximum strain failure criterion. According to the research results, the maximum failure strain of aluminum foam in this paper is 0.37 [37].

3. Validation

3.1. Strain Results Verification. The antiexplosion performance of the foam aluminum sandwich board was studied. All tests were conducted in the structure in Figure 5. Figure 5 is the sandwich test device. The cover plate and the bottom plate are Q235 steel with a radius of 70 mm, the thickness of the cover plate is 10 mm, and the bottom plate thickness is 20 mm. The size of aluminum foam is Φ78 mm × H78 mm, and the porosity of aluminum foam is 80%, 85%, and 90%. Each explosion impact test uses the same loading conditions; choose 520 g TNT suspended 250 mm above the center of the cover. The shock wave generated after the charge explodes acts on the cover plate and transmits and compresses the aluminum foam through the cover plate.

Set three strain measurement points on the bottom surface of the bottom plate. Strain gauge $S1$ is located at the center of the bottom surface of the bottom plate. Strain gauges $S2$ and $S3$ are any points on the circle 4.9 cm and 7.7 cm away from the measurement point of $S1$. The deformation of the bottom plate at 4.9 cm and 7.7 cm from the measuring point of the center $S1$ can explore the relationship between the distance and the precursor wave of the explosion. The arrangement of strain gauges is shown in Figure 6.

As shown in Figure 7, the strain response time-history curve test results of the bottom plate under three porosities are shown. It can be seen from the figure that the strain waveform of the bottom plate under the three porosities has similar regular characteristics, and the strain reaches the maximum value in the first cycle of the response, and the duration of the first response cycle is about 2.5 ms. After the first cycle, the deformation of the bottom plate gradually decreases; the peak strain value from the $S1$ to $S3$ points decreases with the increase of the propagation distance. With the increase of porosity, the maximum peak value of the strain at each measurement point has increased. The increase of strain of 80%–85% is lower than 85%–90%, indicating that the porosity increases to a certain level, due to the explosion load. The fluid-solid coupling effect with the sandwich structure is enhanced, and the energy absorption effect of the aluminum foam is increased, resulting in increased strain.

Figure 8 shows the simulation results of the maximum effective strain time-history curve at each measuring point on the bottom surface of the bottom plate under three porosities. From the figure, the simulation results of the strain time-history curve are consistent with the test results. Under the three porosities, the time interval for the wave head to reach each aluminum foam plate increases slowly. The wave speed of the elastic precursor decreases with the increase of the propagation distance. The strain value at the $S1$ measuring point is the largest, and the vertical distance from the burst center increases. Largely, the strain value of the measuring points of $S2$ and $S3$ keeps decreasing, and the waveforms of the three measuring points are similar to $S1$. As the porosity increases, the strain value at each measuring point increases, indicating that as the porosity increases, the aluminum foam effectively shares the explosive load and plays the role of antiexplosion and wave elimination, which reduces the deformation of the bottom plate. Further research on the design of explosive vessels provides a theoretical basis.

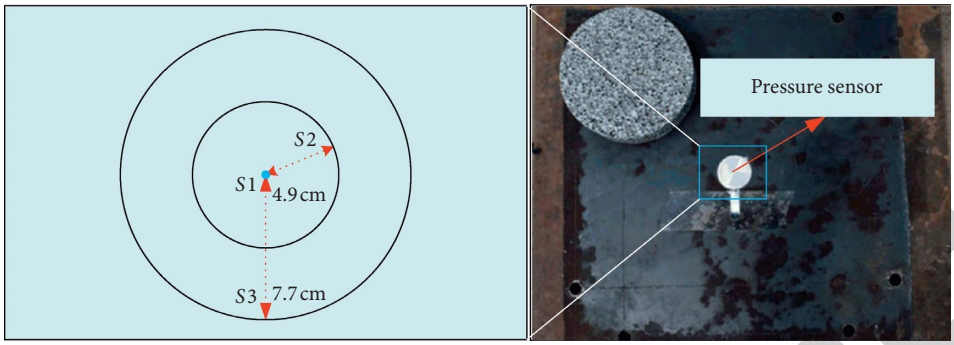

Figure 6: Sensor layout.

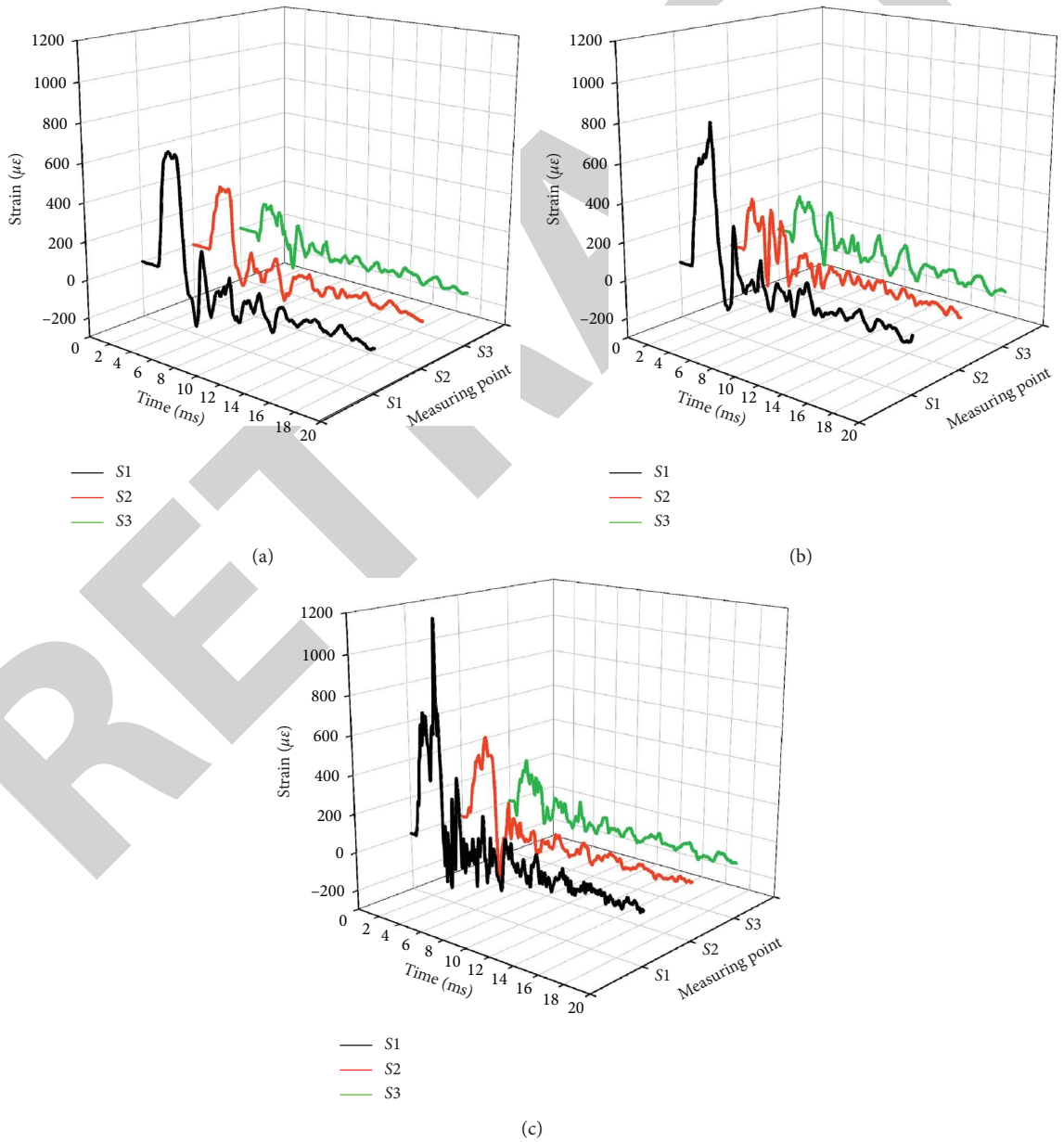

Figure 7: Time-history curve of strain response of bottom plate under different porosity under test. (a) 80%. (b) 85%. (c) 90%.

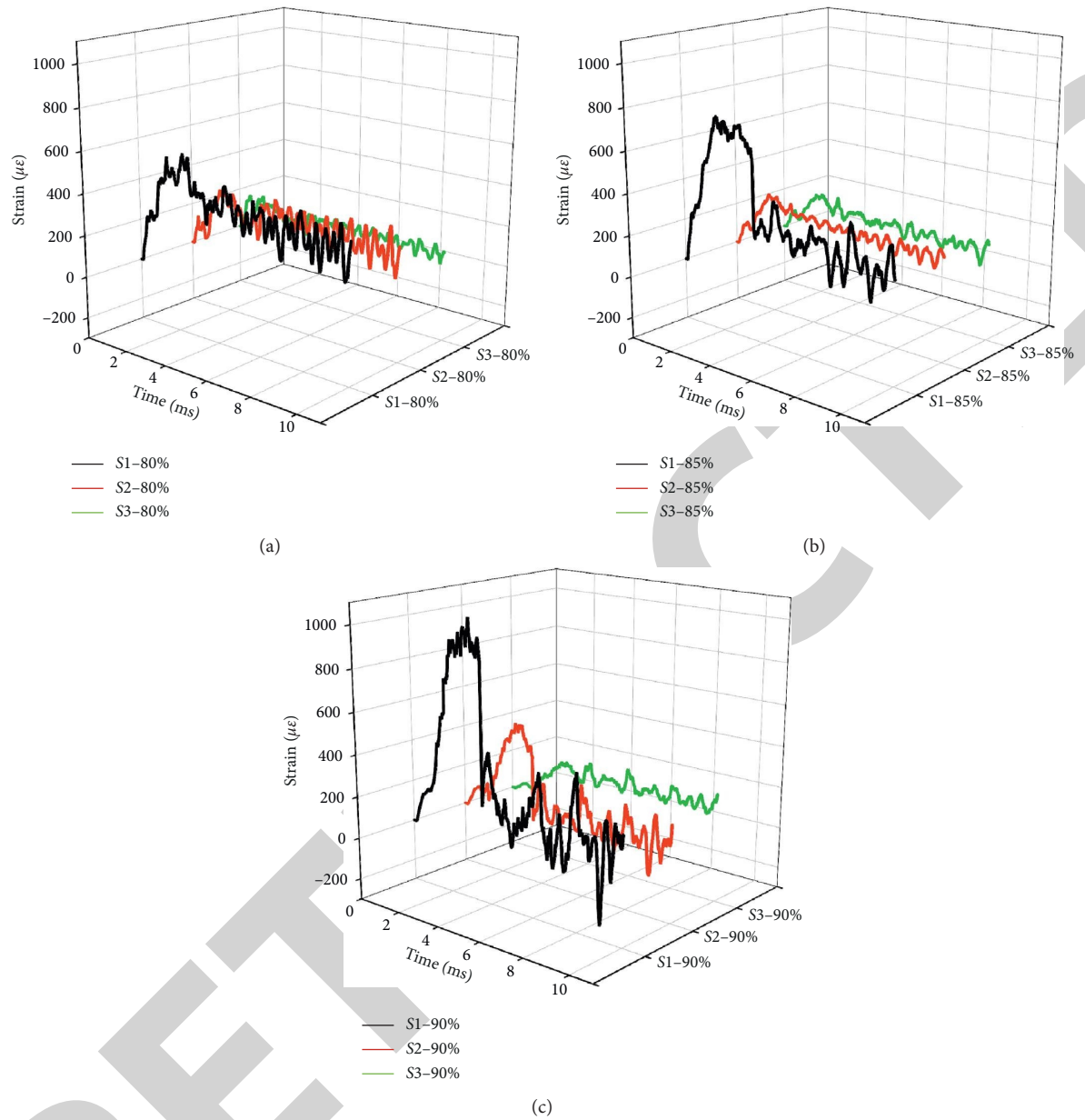

Figure 8: Strain time-history curve of each measuring point under different porosity under simulation. (a) 80%. (b) 85%. (c) 90%.

Figure 9 is a comparison chart of the numerical simulation results and test results of the peak strain values of the three groups of porosity aluminum foam under the explosive shock wave of the charge. In order to quantitatively describe the difference between the test and the numerical simulation, the numerical simulation results of the strain at each measuring point of the bottom plate are taken as the x-axis, and the test results are taken as the y-axis, and Figure 9 is drawn. The line with a slope of 1 in the figure indicates that the numerical simulation results are completely consistent with the test results. When the test point falls below the straight line, it means that the measured strain given by the numerical simulation is greater than the test value; when the test point falls above the straight line, it indicates that the peak value of strain at each measuring point calculated by numerical simulation is smaller than the test value. It can be intuitively seen from Figure 9 that the test points basically fall between the solid line with a slope of 1 and the broken line with a slope of 0.90 and 1.1, and the error is within 10%. The numerical simulation results of the strain values at different measuring points under different porosities are in good agreement with the experimental results, indicating that the simulation results are good and verify the correctness of the three-dimensional mesoscopic model of aluminum foam.

3.2. Comparison of Structural Forms. Figure 10 is the internal structure of aluminum foam, Figure 10(a) is the macrostructure of aluminum foam in its natural state, Figure 10(b) is the morphology of 85% aluminum foam after electron

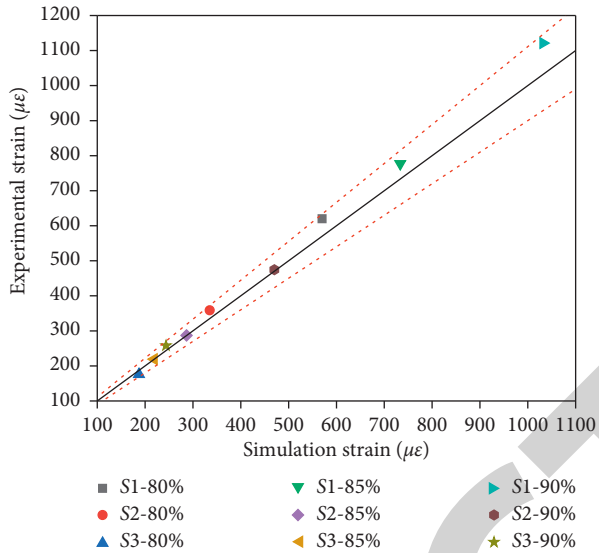

Figure 9: Comparison graph of numerical simulation and test results.

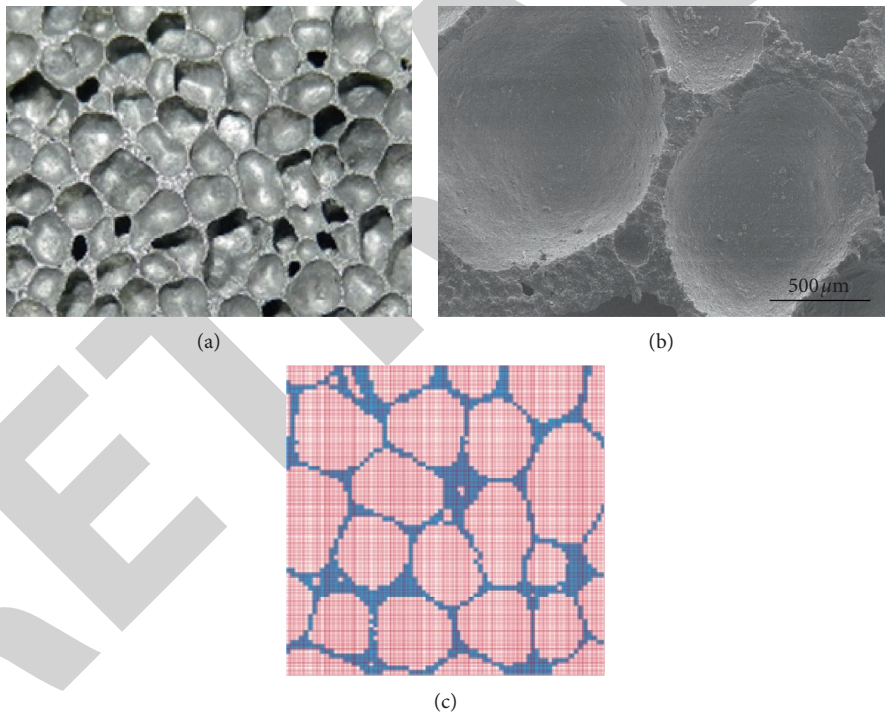

Figure 10: The real structure and numerical simulation structure of aluminum foam.

microscopy, and Figure 10(c) is a three-dimensional mesomodel, modeling 85% porosity aluminum foam structure. In order to verify the reliability of the structural form of the model, three slices were taken in the established three-dimensional mesomodel, the number of cell units and air units were counted, and the porosity of each slice was calculated and compared with the porosity of real aluminum foam. For comparison, the results are shown in Figure 11. It can be seen from the figure that the porosity of different slices in the model is in good agreement with the real aluminum foam structure, with a maximum difference of 4.42%. The comprehensive strain comparison finally concluded that the agreement between the numerical simulation and the test can reach more than 91.4%. It shows that the established model can accurately express the mesoscopic structural characteristics of aluminum foam, and the modeling results are reliable. It can be observed that the structure with greater porosity has thicker cell walls.

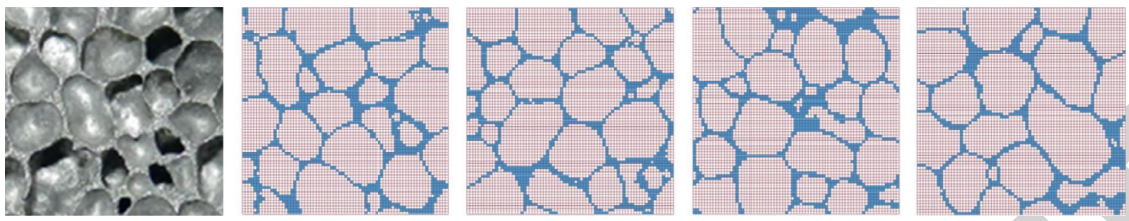

Figure 11: Comparison of different sections of the model with the real structure.

4. Analysis of Mesoresults

4.1. Analysis of Aluminum Foam Movement Process under Blast Loading. This section explores the movement of an aluminum foam sandwich panel with a porosity of 80% under explosive load.

In the first stage, the explosive center detonated until the shock wave reached the cover and began to compress the aluminum foam. As shown in Figure 12, at 0 ms, the explosive performs a single-point center detonation, and the shock wave front starts to expand outwards with the sphere as the center and reaches the cover plate at a certain time between 0.07 ms and 0.08 ms. At a certain speed, the aluminum foam is compressed downward, as shown in the pressure cloud diagram of the aluminum foam on the right side of Figure 12.

Figure 13 shows the process of compressing aluminum foam after the plane spherical wave reaches the cover. At 0.08 ms, the stress wave starts to propagate in the aluminum foam. At 0.09 ms, the stress wave has propagated to the bottom of the aluminum foam and transmitted the stress wave to the bottom plate, and the bottom plate has undergone a stress change. Subsequently, the foamed aluminum experienced significant plastic strain, and the cell walls began to deform and break down. At 0.429 ms, the deformation of the hole wall reached saturation, and the hole wall collapsed and destroyed. At 1.4 ms, the foam aluminum stops deforming, and the entire compression process of the aluminum foam is initially completed.

In order to explore the antiexplosion and wave attenuation capabilities of aluminum foam, we have quantitatively analyzed the attenuation effect of the stress wave strength of the aluminum foam sandwich structure through the three-dimensional mesoscopic model of the aluminum foam, taking the first layer of aluminum foam at different porosities. The average stress of the element is taken as σ_1, and the stress value of the foam aluminum introduced into the cover plate is obtained. The average stress of the uppermost unit of the bottom plate is taken as σ_2, and the stress value of the bottom plate after the explosion wave passes through the aluminum foam is obtained. The distribution of stress waves in the sandwich structure is shown in Figure 14. In the initial stage, stress concentration occurs in local weak areas, the cell walls are in an elastic state, and the stress level rises rapidly with strain. Intuitively, the stress value of 80% porosity aluminum foam in Figure 14(a) reaches 184.34 MPa at 0.4 ms, and the stress wave intensity at the bottom of the bottom plate after passing the aluminum foam is 2.45 MPa. It can be seen that the blast shock wave decays up to 98.67% after passing through the foamed aluminum. As shown in Figure 14(b), when the porosity of the aluminum foam upper layer is 85%, the stress value reaches 147.35 MPa at 0.384 ms, and the stress wave intensity at the bottom of the bottom plate after passing the aluminum foam is 1.61 MPa. It can be seen that the blast shock wave attenuation is as high as 98.91% after passing through the aluminum foam. As shown in Figure 14(c), when the porosity of the aluminum foam upper layer is 90%, the stress value reaches 86.03 MPa at 0.149 ms, and the stress wave strength at the bottom of the bottom plate after passing the aluminum foam is 4.09 MPa. It can be seen that the explosion shock wave attenuation is as high as 95.25% after passing through the aluminum foam.

It can be concluded that as the porosity increases, the stress value of the cover plate transmitted to the aluminum foam decreases significantly, but the stress value of the bottom plate increases first as the porosity decreases.

The relationship between the foam aluminum with different porosities and the wave elimination rate is shown. As shown in Figure 15, the wave elimination ability of aluminum foam does not increase with the increase of porosity, but there is an extreme value. Probably between 83% and 84% porosity, before reaching the threshold, its antiknocking ability will increase with the increase of porosity, but after reaching the threshold, its antiknocking ability will decrease with the increase of porosity.

4.2. Mechanism Analysis. Figure 16 shows the effective plastic strain of the foam aluminum cell wall under the blast load. It can be seen that, at 80% porosity, the deformation is concentrated in local weak areas, and the cell walls are in an elastic state. When the porosity becomes 85%, the cell wall breaks. The cell wall deformation indicates that plastic strain consumes a lot of energy under dynamic load. As the deformation further increases, the local plastic deformation of the unit increases rapidly, and the stress reaches the bearing capacity and breaks, resulting in the generation of some weak surfaces and the formation of a single failure penetration area. As the porosity increases, the aluminum foam has stress concentration, the cell wall collapses, the plastic strain of the aluminum foam cell wall mainly occurs in the upper region, and the lower part of the aluminum foam collapses and compacts.

To explore the mechanism, we conducted an electron microscopy scan of the aluminum foam to explore its microscopic properties. Figure 17(a) shows the typical failure

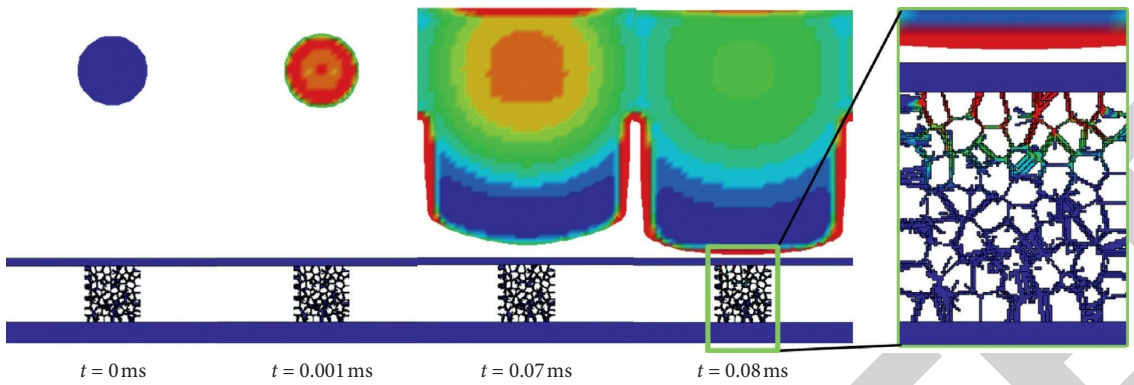

Figure 12: Explosion shock wave reaches the cover plate and begins to compress the aluminum foam.

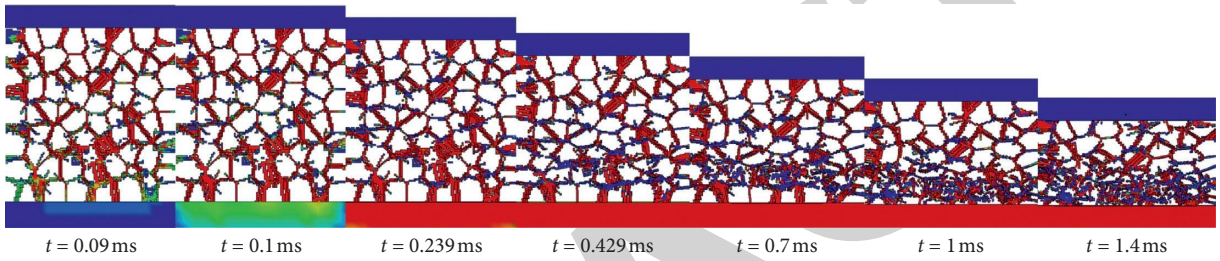

Figure 13: Cloud image of foam aluminum compression process.

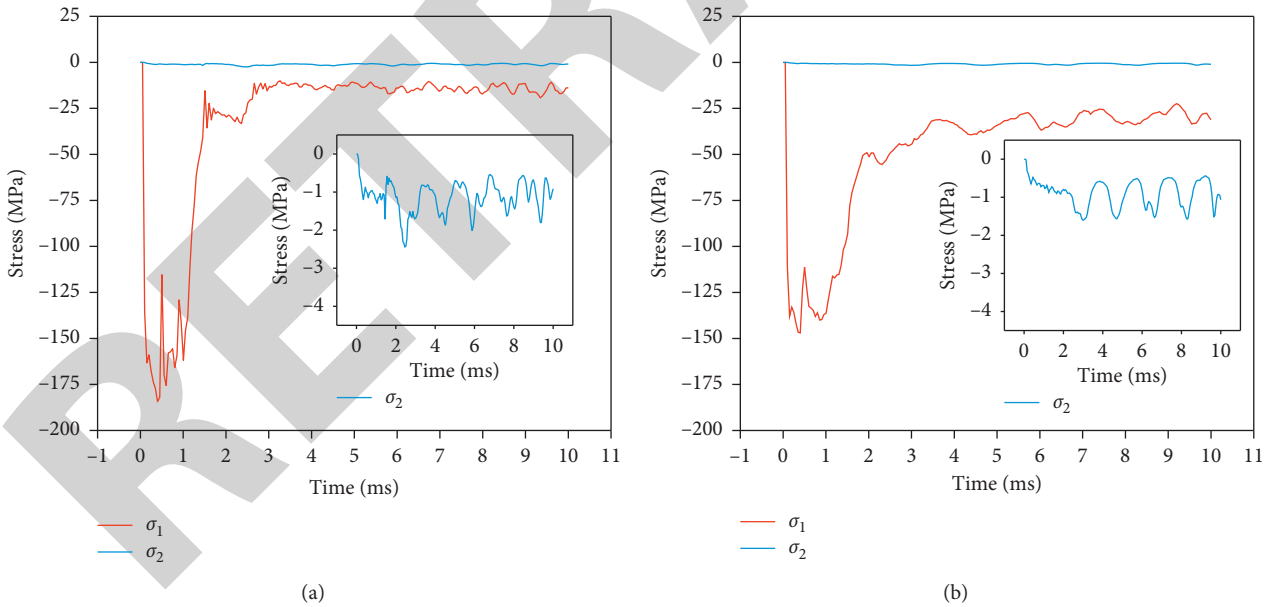

Figure 14: Continued.

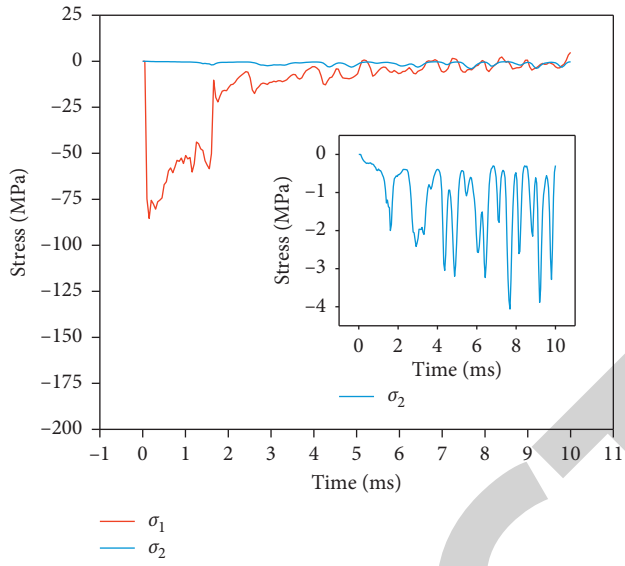

(c)

Figure 14: Stress-time curve of aluminum foam under different porosities. (a) 80%. (b) 85%. (c) 90%.

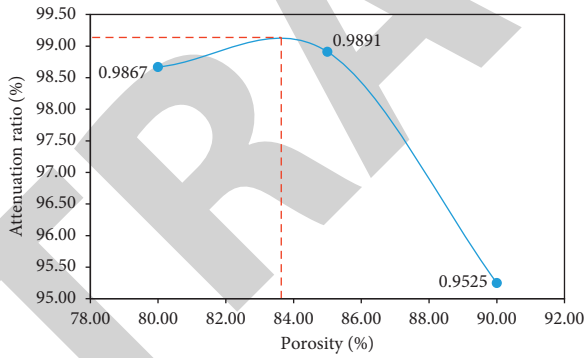

Figure 15: Wave elimination rate curve of aluminum foam under different porosity.

mode of aluminum foam after 85% of the sandwich structure is subjected to explosion impact. According to the results of electron microscope scanning (SEM) experiments (b-e), the microscopic morphological changes of the cells and cell walls of aluminum foam were demonstrated. Figure 16(b) shows the original state of the aluminum foam cell wall. Under the blast load, both the cover and the panel in the sandwich structure undergo large plastic deformation, and the obvious "X"-shaped failure zone appears in the aluminum foam material. According to the scanning electron microscopy results, the deformation of aluminum foam can be divided into four areas: area I, elastic deformation area, the cell structure has not changed significantly as shown in Figure 17(b); area II, the cell wall has undergone significant plastic deformation as shown in Figure 17(c); area III, the cell wall breaks and the structure is destroyed as shown in Figure 17(d); area IV, the cell wall begins to collapse and is gradually compacted as shown in Figure 17(e).

Figure 18 shows the microscopic morphology of aluminum foam under different porosity after explosion. To ensure the single variability, the center position of aluminum foam under different porosity was selected for electron microscopy scanning. It can be seen from the figure that, with the increase of porosity, the complete pores in the aluminum foam decrease; when the porosity is 85%, the collapse of the pores in the aluminum foam is obvious, the complete pores are almost absent, and the pores are compressed. At% porosity, no complete pores can be seen inside the foam aluminum, and the degree of pore compression is significantly higher than that of the foam aluminum at 85% porosity. It can be seen that the increase in porosity will change the microstructure of aluminum foam. The greater the porosity, the deeper the degree of pore damage.

When subjected to an impact load, aluminum foam is extremely susceptible to deformation. Because aluminum foam is a porous structure, transmission and reflection occur during the propagation of an explosion wave, so there is more reflection, and a part of energy is well converted into internal energy and kinetic energy. Through the study of the mesoscopic model of aluminum foam cell walls, it is found

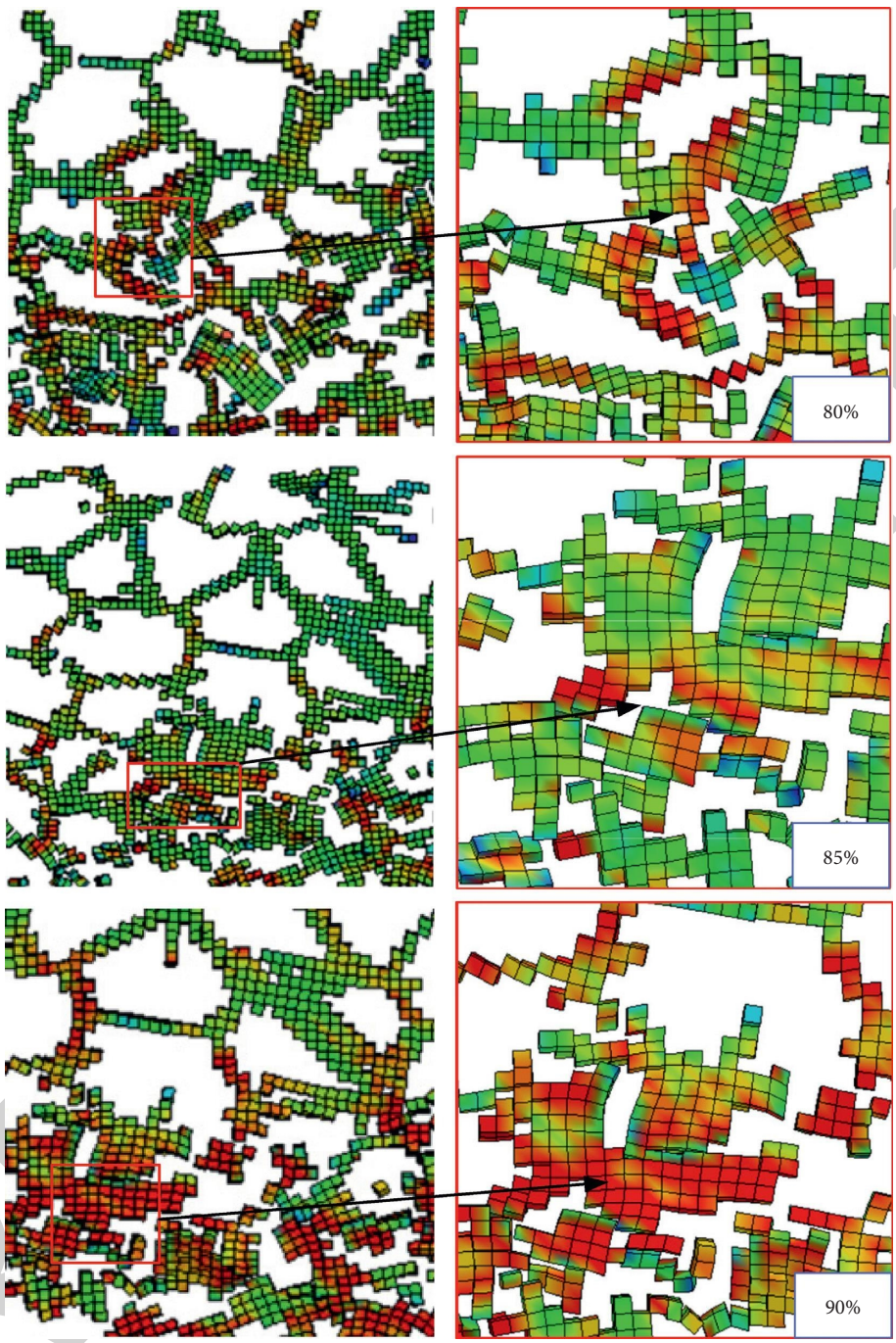

Figure 16: Cell wall collapse and rupture.

that the energy absorption of aluminum foam mainly consumes energy through various forms such as crushing, deformation, fracture, and mutual friction of the pore walls of the aluminum foam, so as to achieve the effect of energy absorption. When the porosity is increased to about 85%, the energy absorption effect of aluminum foam is saturated, and the porosity continues to increase so that the aluminum foam is compacted to produce stress enhancement, so the load pressure on the bottom plate increases instead. Under a certain explosion load, the explosion stress wave transmits and propagates through the solid medium of the cell wall or between the bubbles and the solid. Due to the structural characteristics of random cell generation of aluminum foam, stress waves propagate in the constantly changing solid medium and the interference of reflection and transmission in the bubbles rapidly attenuates. When the stress wave peak is greater than the cell wall strength, deformation and destruction occur. As the propagation distance increases, the stress wave peak decreases and the amount of deformation also weakens until elastic deformation occurs. Therefore, the antiexplosion performance of foamed aluminum is directly related to the cell wall thickness and the size of bubbles.

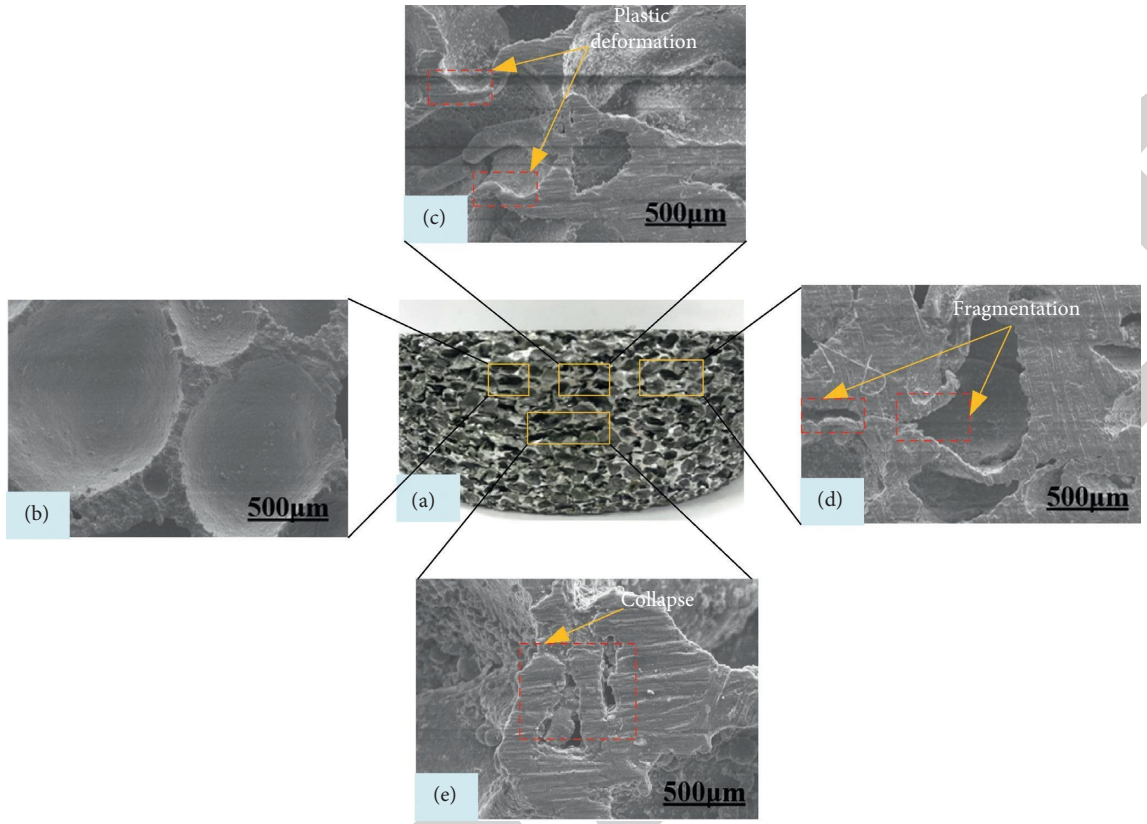

Figure 17: Wave elimination rate curve of aluminum foam under different porosity.

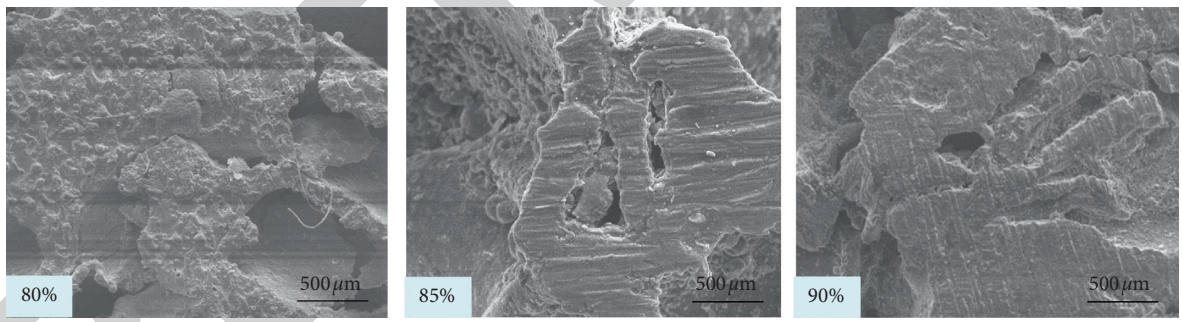

Figure 18: Microstructure of aluminum foam under different porosities.

Under a certain load, the contribution of the two to anti-explosion will also change. For example, after the porosity reaches the extreme value of 83%-84%, the deformation energy absorption of the cell wall is more obvious than that of the bubble. The cell wall thickness of 85% aluminum foam is greater than 90%.

5. Conclusion

In this paper, the explosive impact test was carried out under the explosive quantity of 520 g and the explosion height of 25 cm. The attenuation law of stress wave in the aluminum foam sandwich plate was studied, and the strain response characteristics of the bottom plate were analyzed. In addition, a three-dimensional mesomodel for the finite element analysis of aluminum foam is established. On the basis of the three-dimensional micromechanical model, the influence of the micromechanical structure (porosity) of aluminum foam is considered, and the performance of aluminum foam under the blast impact load is studied. The following conclusions can be drawn:

(1) Based on the Voronoi algorithm, firstly, the 2-random polyhedron model is established by using ABAQUS, and its geometric features are extracted. Then, by using Python language and Fortran language synthetically, the algorithm of generating aluminum foam with random pore size and wall thickness is written, and the grid model is established

by the algorithm read in by TrueGrid software. Finally, the part of the particles is removed to generate the aluminum foam model. Then, the energy absorption mechanism and porosity of the sandwich structure with aluminum foam core are explored under the action of explosion load, and the reliable results can be obtained, which are in good agreement with the test results.

(2) Through the electron microscope test, it is found that the plastic strain is mainly concentrated in the upper region of aluminum foam under the action of explosion load, and there is an obvious "X" type failure zone in the material of aluminum foam. According to the SEM results, the deformation of aluminum foam is divided into four regions: elastic deformation region, plastic deformation region, cell wall fracture region, and collapse region.

(3) Through the microscopic simulation of aluminum foam, it is found that the main reasons for aluminum foam antiknock are the deformation and destruction of the cell wall, the propagation of stress wave corresponding to the cell wall, the multiple reflections, and transmission of stress wave corresponding to bubble. Cell wall thickness and bubble size are some of the key parameters of antiknock performance.

(4) Based on the simulation results, it is found that the porosity has a significant impact on the antiknock ability of aluminum foam, and the porosity has an extreme value of about 83% to 84% for antiknock ability. With the increase of porosity, the strain value of each measuring point of the bottom plate increases, which can absorb more energy, but it increases the energy transfer from the explosion load to the sandwich structure and makes the load amplitude acting on the bottom plate larger.

Data Availability

The drawings and tables in the article are all original data, which are all obtained by experiments and computer simulations. In the future, when readers need the data in the article for secondary development, they can e-mail the corresponding author to provide it. The drawings and tables in the article can be edited without any problems.

Disclosure

The authors declare that they have no financial and personal relationships with other people or organizations that can inappropriately influence their work.

Conflicts of Interest

The authors declare that they have no conflicts of interest.

Acknowledgments

The financial support from the Science and Technology Innovation Project (KYGYZB0019003) and the Department of Infrastructure Barracks (China) is gratefully acknowledged.

References

[1] M. F. Ashby, A. G. Evans, N. A. Fleck et al., "Metal foams: A design guide," *Applied Mechanics Reviews*, vol. 23, no. 6, p. 119, 2012.

[2] A. G. Evans, J. W. Hutchinson, and M. F. Ashby, "The topological design of multifunctional cellular metals," *Progress in Materials Science*, vol. 43, p. 171, 1999.

[3] G. W. Ma and Z. Q. Ye, "Analysis of foam claddings for blast alleviation," *International Journal of Impact Engineering*, vol. 34, no. 1, pp. 60–70, 2007.

[4] A. G. Evans, J. W. Hutchinson, N. A. Fleck, M. F. Ashby, and H. N. G. Wadley, "The topological design of multifunctional cellular metals," *Progress in Materials Science*, vol. 46, no. 3-4, pp. 309–327, 2001.

[5] J. Banhart, "Manufacture, characterisation and application of cellular metals and metal foams," *Progress in Materials Science*, vol. 46, no. 6, pp. 559–632, 2001.

[6] Y. Xia, C. Wu, Z. Liu et al., "Protective effect of graded density aluminium foam on RC slab under blast loading–An experimental study," *Construction and Building Materials*, vol. 111, pp. 209–222, 2016.

[7] S. Wang, Y. Ding, C. Wang, Z. Zheng, and J. Yu, "Dynamic material parameters of closed-cell foams under high-velocity impact," *International Journal of Impact Engineering*, vol. 99, pp. 111–121, 2017.

[8] N. Movahedi and S. M. H. Mirbagheri, "Comparison of the energy absorption of closed-cell aluminum foam produced by various foaming agents," *Strength of Materials*, vol. 48, no. 3, pp. 444–449, 2016.

[9] A. Jung, E. Lach, and S. Diebels, "New hybrid foam materials for impact protection," *International Journal of Impact Engineering*, vol. 64, pp. 30–38, 2014.

[10] X. R. Liu, X. G. Tian, T. J. Lu, and B. Liang, "Sandwich plates with functionally graded metallic foam cores subjected to air blast loading," *International Journal of Mechanical Sciences*, vol. 84, pp. 61–72, 2014.

[11] R. Sriram, U. K. Vaidya, and J. E. Kim, "Blast impact response of aluminum foam sandwich composites," *Journal of Materials Science*, vol. 41, no. 13, pp. 4023–4039, 2006.

[12] M. D. Goel, P. Altenhofer, V. A. Matsagar, A. K. Gupta, C. Mundt, and S. Marburg, "Interaction of a shock wave with a closed cell aluminum metal foam," *Combustion, Explosion, and Shock Waves*, vol. 51, no. 3, pp. 373–380, 2015.

[13] J. Shen, G. Lu, Z. Wang, and L. Zhao, "Experiments on curved sandwich panels under blast loading," *International Journal of Impact Engineering*, vol. 37, no. 9, pp. 960–970, 2010.

[14] L. Jing, Z. Wang, V. P. W. Shim, and L. Zhao, "An experimental study of the dynamic response of cylindrical sandwich shells with metallic foam cores subjected to blast loading," *International Journal of Impact Engineering*, vol. 71, pp. 60–72, 2014.

[15] Z. Wang, L. Jing, J. Ning, and L. Zhao, "The structural response of clamped sandwich beams subjected to impact loading," *Composite Structures*, vol. 93, no. 4, pp. 1300–1308, 2011.

[16] F. Zhu, L. Zhao, G. Lu, and Z. Wang, "Deformation and failure of blast-loaded metallic sandwich panels-experimental investigations," *International Journal of Impact Engineering*, vol. 35, no. 8, pp. 937–951, 2008.

[17] Y. Feng, Z. Zhu, and S. Hu, "Dynamic compressive behavior of aluminum alloy foams," *Journal of Materials Science Letters*, vol. 20, no. 18, pp. 1667-1668, 2001.

[18] Y. An, C. Wen, P. D. Hodgson, and C. Yang, "Investigation of cell shape effect on the mechanical behaviour of open-cell metal foams," *Computational Materials Science*, vol. 55, pp. 1–9, 2012.

[19] K. Li, X.-L. Gao, and G. Subhash, "Effects of cell shape and strut cross-sectional area variations on the elastic properties of three-dimensional open-cell foams," *Journal of the Mechanics and Physics of Solids*, vol. 54, no. 4, pp. 783–806, 2006.

[20] S. Santosa and T. Wierzbicki, "On the modeling of crush behavior of a closed-cell aluminum foam structure," *Journal of the Mechanics and Physics of Solids*, vol. 46, no. 4, pp. 645–669, 1998.

[21] C. Chen, T. J. Lu, and N. A. Fleck, "Effect of inclusions and holes on the stiffness and strength of honeycombs," *International Journal of Mechanical Sciences*, vol. 43, no. 2, pp. 487–504, 2001.

[22] C. Y. Zhang, L. Q. Tang, B. Yang, L. Zhang, X. Q. Huang, and D. N. Fang, "Meso-mechanical study of collapse and fracture behaviors of closed-cell metallic foams," *Computational Materials Science*, vol. 79, pp. 45–51, 2013.

[23] D. Karagiozova, G. N. Nurick, and G. S. Langdon, "Behaviour of sandwich panels subject to intense air blasts–Part 2: Numerical simulation," *Composite Structures*, vol. 91, no. 4, pp. 442–450, 2009.

[24] L. J. Gibson and M. F. Ashby, *Cellular Solids: Structure and Properties*, Cambridge University Press, Cambridge, U. K, 1999.

[25] K. Li, X.-L. Gao, and A. K. Roy, "Micromechanics model for three-dimensional open-cell foams using a tetrakaidecahedral unit cell and Castigliano's second theorem," *Composites Science and Technology*, vol. 63, no. 12, pp. 1769–1781, 2003.

[26] M. Laroussi, K. Sab, and A. Alaoui, "Foam mechanics: Nonlinear response of an elastic 3D-periodic microstructure," *International Journal of Solids and Structures*, vol. 39, no. 13-14, pp. 3599–3623, 2002.

[27] N. J. Mills, "The high strain mechanical response of the wet Kelvin model for open-cell foams," *International Journal of Solids and Structures*, vol. 44, no. 1, pp. 51–65, 2007.

[28] K. Tunvir, A. Kim, and S. S. Cheon, "Analytical solution for crushing behavior of closed cell al-alloy foam," *Mechanics of Advanced Materials and Structures*, vol. 14, no. 5, pp. 321–327, 2007.

[29] L. Li, P. Xue, Y. Chen, and H. S. U. Butt, "Insight into cell size effects on quasi-static and dynamic compressive properties of 3D foams," *Materials Science and Engineering: A*, vol. 636, pp. 60–69, 2015.

[30] G. W. Ma, Z. Q. Ye, and Z. S. Shao, "Modeling loading rate effect on crushing stress of metallic cellular materials," *International Journal of Impact Engineering*, vol. 36, no. 6, pp. 775–782, 2009.

[31] Z. Zheng, C. Wang, J. Yu, S. R. Reid, and J. J. Harrigan, "Dynamic stress–strain states for metal foams using a 3D cellular model," *Journal of the Mechanics and Physics of Solids*, vol. 72, pp. 93–114, 2014.

[32] Q. Fang, J. Zhang, Y. Zhang, H. Wu, and Z. Gong, "A 3D mesoscopic model for the closed-cell metallic foams subjected to static and dynamic loadings," *International Journal of Impact Engineering*, vol. 82, pp. 103–112, 2015.

[33] Q. Fang, J. Zhang, Y. Zhang et al., "Mesoscopic investigation of closed-cell aluminum foams on energy absorption capability under impact," *Composite Structures*, vol. 124, pp. 409–420, 2015.

[34] D. Weaire, J. P. Kemrode, and J. Wejchert, "On the distribution of cell areas in a Voronoi network," *Philosophical Magazine B*, vol. 53, no. 5, pp. L101–L105, 1986.

[35] D. Shi, Y. Li, and S. Zhang, *Explicit Dynamic Analysis Based on ANSYS/LS-DYNA*, Tsinghua University Press, Beijing, China, 2005.

[36] V. R. Feldgun, Y. S. Karinski, I. Edri, and D. Z. Yankelevsky, "Prediction of the quasi-static pressure in confined and partially confined explosions and its application to blast response simulation of flexible structures," *International Journal of Impact Engineering*, vol. 90, no. 15, pp. 46–60, 2016.

[37] H.-W. Song, Q.-J. He, J.-J. Xie, and A. Tobota, "Fracture mechanisms and size effects of brittle metallic foams: in situ compression tests inside SEM," *Composites Science and Technology*, vol. 68, no. 12, pp. 2441–2450, 2008.